Plant hydraulic modelling of leaf and canopy fuel moisture content reveals increasing vulnerability of a Mediterranean forest to wildfires under extreme drought

Julien Ruffault[1] , Jean-Marc Limousin[2] , François Pimont[1] , Jean-Luc Dupuy[1] , Miquel De Càceres[3] , Hervé Cochard[4] , Florent Mouillot[2] , Chris J. Blackman[5] , José M. Torres-Ruiz[4] , Russell A. Parsons[6] , Myriam Moreno[1] , Sylvain Delzon[7] , Steven Jansen[8] , Albert Olioso[1] , Brendan Choat[9] and Nicolas Martin-StPaul[1]

[1]URFM, INRAE, 84000 Avignon, France; [2]CEFE, Univ Montpellier, CNRS, EPHE, IRD, 34000 Montpellier, France; [3]CREAF, Bellaterra (Cerdanyola del Vallès), E08193, Catalonia, Spain; [4]Université Clermont-Auvergne, INRAE, PIAF, 63000 Clermont-Ferrand, France; [5]School of Biological Sciences, University of Tasmania, Hobart, Tas. 7001, Australia; [6]Fire Sciences Laboratory, Rocky Mountain Research Station, USDA Forest Service, Missoula, MT 59808, USA; [7]Univ. Bordeaux, INRAE, BIOGECO, 33615, Pessac, France; [8]Institute of Systematic Botany and Ecology, Ulm University, D-89081, Ulm, Germany; [9]Western Sydney University, Penrith, NSW 2751, Australia

Summary

- Fuel moisture content (FMC) is a crucial driver of forest fires in many regions world-wide. Yet, the dynamics of FMC in forest canopies as well as their physiological and environmental determinants remain poorly understood, especially under extreme drought.

- We embedded a FMC module in the trait-based, plant-hydraulic *SurEau-Ecos* model to provide innovative process-based predictions of leaf live fuel moisture content (LFMC) and canopy fuel moisture content (CFMC) based on leaf water potential (ψ_{Leaf}). *SurEau-Ecos-FMC* relies on pressure–volume (p-v) curves to simulate LFMC and vulnerability curves to cavitation to simulate foliage mortality.

- *SurEau-Ecos-FMC* accurately reproduced ψ_{Leaf} and LFMC dynamics as well as the occurrence of foliage mortality in a Mediterranean *Quercus ilex* forest. Several traits related to water use (leaf area index, available soil water, and transpiration regulation), vulnerability to cavitation, and p-v curves (full turgor osmotic potential) had the greatest influence on LFMC and CFMC dynamics. As the climate gets drier, our results showed that drought-induced foliage mortality is expected to increase, thereby significantly decreasing CFMC.

- Our results represent an important advance in our capacity to understand and predict the sensitivity of forests to wildfires.

Introduction

Wildfires have grown in size and intensity in several regions due to anthropogenic climate change (Jones *et al.*, 2022). Increased atmospheric aridity (Grossiord *et al.*, 2020), sometimes combined with decreased precipitation (Dai, 2013), has decreased vegetation moisture and contributed to rises in burnt areas (Abatzoglou & Williams, 2016; Ellis *et al.*, 2022; Rao *et al.*, 2022) and extreme wildfires (Ruffault *et al.*, 2018a; Nolan *et al.*, 2020b; Duane *et al.*, 2021). Yet, the temporal and spatial dynamics of fuel moisture across vegetation types and species, as well as their physiological or environmental determinants, remain largely unknown, especially under extreme drought conditions. As compound dry and hot events become more frequent and intense (Alizadeh *et al.*, 2020; Ruffault *et al.*, 2020), understanding and anticipating fire hazard require an improvement to our current knowledge of vegetation moisture response to climate.

Fuel moisture content (FMC), the ratio of water mass to dry mass of vegetation, governs the amount of time and energy needed to vaporize fuel moisture before ignition can occur and is an important meteorological-driven driver of fire activity and behavior. Fuel moisture content is usually separated into dead fuel moisture content (DFMC) and live fuel moisture content (LFMC) components, whose relative roles in driving wildfire behavior remain widely debated across fire regimes and ecosystems (Yebra *et al.*, 2013; Resco de Dios *et al.*, 2022). Nonetheless, declining LFMC was associated with an increase in area burned (Chuvieco *et al.*, 2009; Dennison & Moritz, 2009; Nolan *et al.*, 2016; Pimont *et al.*, 2019a; Rao *et al.*, 2022) and fire intensity (Rossa *et al.*, 2016; Pimont *et al.*, 2019b; Banerjee *et al.*, 2020) in midlatitude forests and shrublands. Numerous findings also point out the impact of long-lasting drought on wildfire activity (Turco *et al.*, 2017; Ruffault *et al.*, 2020; Abram *et al.*, 2021), indirectly highlighting the role of fuel moisture of

slow-responding fuel compartments in the occurrence of the largest fire events.

Despite its importance for wildfire hazard, the dynamics of LFMC during drought remain poorly understood and predicted, largely because, unlike DFMC, the effect of climate on LFMC is regulated by a range of location-specific factors, including plant traits and soil characteristics (Nolan *et al.*, 2018, 2020a; Ruffault *et al.*, 2018b; Pivovaroff *et al.*, 2019; Scarff *et al.*, 2021). As a result, models based only on meteorological drought indices are often unable to accurately predict LFMC because they do not take species-specific plant physiology into account (Ruffault *et al.*, 2018b). Recent progress in remotely sensed approaches, including spectral vegetation indices (Yebra *et al.*, 2013), radiative transfer models (Yebra *et al.*, 2018; Marino *et al.*, 2020), and microwave-based methods (Fan *et al.*, 2018; Rao *et al.*, 2020), has improved our understanding of LFMC patterns of variation. Nevertheless, remote sensing provides limited insights into physiological mechanisms involved in LFMC dynamics and suffers from its limited temporal scope.

Another obstacle to LFMC predictions is the ambiguity in its definition, which vary across scientific disciplines and/or the spatial scale of the study. Live fuel moisture content is usually defined as the moisture content of the living material at a leafy shoot level in ecophysiological studies, thereby matching the scale of laboratory measurements (Martin-StPaul *et al.*, 2018). By contrast, studies based on remote sensing techniques provide estimations of equivalent water thickness, which is closer to the canopy fuel moisture content (CFMC; Yebra *et al.*, 2013; Chakroun *et al.*, 2015). Indeed, the equivalent water thickness is also sensitive to the LFMC of shoots and other small woody components at the top of the canopy and integrates the impact of canopy partial mortality. Canopy fuel moisture content is therefore more relevant for assessing wildfire danger because it integrates the moisture of the entire vegetation layer. Main differences between LFMC and CFMC arise when leaf or branch dieback occurs within the canopy and transforms live fuel into dead fuel (Ruthrof *et al.*, 2016; Nolan *et al.*, 2020a). Because the moisture content of dead fuels is well below that of live fuels, the differences between measurements of LFMC and estimates of CFMC increase as the ratio of dead-to-live fuel (α_{Dead}) increases in the canopy. As the climate warms, accumulating evidence shows that drought-induced plant mortality and leaf damage increase in many ecosystems (Allen *et al.*, 2015; Hammond *et al.*, 2022). Such events are expected to decrease fuel moisture and exacerbate the probability and intensity of crown fires.

Recent advances in our physiological understanding of plant response to drought have led to new opportunities to improve our comprehension of LFMC and CFMC sensitivity to drought. We can describe the dependence of LFMC and CFMC to plant drought by combining two different ecophysiological frameworks (Fig. 1), which both rely on the assumption that leaf water potential (ψ_{Leaf}) is a relevant indicator of plant's exposure to drought. A first theoretical framework is derived from pressure–volume (*p-v*) curves. It states that the response of symplasmic water content to leaf water potential (ψ_{Leaf}) essentially depends on cell wall elasticity (ε) and leaf osmotic potential (π_0; Tyree & Hammel, 1972;

Bartlett *et al.*, 2012). Such relationships have recently been adapted to model leaf LFMC (Nolan *et al.*, 2020a; Scarff *et al.*, 2021). A second framework, also inherited from plant hydraulics, formulates the water content of the apoplasmic tissue and the ratio of dead-to-live fuels within the canopy to (α_{Dead}) as a function of the percent loss of leaf hydraulic conductance (PLC). PLC is derived from the vulnerability curve to cavitation and can be directly related to the water discharge from the apoplasm compartments (Hölttä *et al.*, 2009; Martin-StPaul *et al.*, 2017). PLC is also a measure of hydraulic failure, which has been shown to relate to foliage mortality (Hammond *et al.*, 2019; Cardoso *et al.*, 2020; Klein *et al.*, 2022), and can thus be used to estimate the fraction of foliage that turns dead during drought. The plant's exposure to drought (ψ_{Leaf}), used in both frameworks, can be simulated by plant-hydraulic models as a function of climate, plant traits, and soil characteristic that drive the water demand and supply during drought, including the leaf area index (LAI), rooting depth, and stomatal conductance response to water potential (ψ_{gs50}).

While the number of plant-hydraulic models is growing rapidly (Tuzet *et al.*, 2017; Couvreur *et al.*, 2018; Kennedy *et al.*, 2019; De Kauwe *et al.*, 2020; Li *et al.*, 2021), only few studies have sought to simulate LFMC (Ma *et al.*, 2021). None, to our knowledge, have attempted to derive CFMC from process-based estimations of LFMC and foliage mortality. Here, we hypothesized that (1) CFMC will decline with climate change because of the increase in drought-induced foliage mortality and that (2) species-specific plant traits related to hydraulic safety, water regulation, and internal stores largely explain fuel moisture response to extreme drought. We developed a FMC module in the plant-hydraulic *SurEau-Ecos* model (Ruffault *et al.*, 2022) to simulate the dynamics of both LFMC and CFMC. We compared these predictions to measurements of fuel moisture and foliage mortality made in a Mediterranean *Quercus ilex* forest site during three consecutive dry summers from 2016 to 2018. We then explored the key parameters and species traits that drive LFMC and CFMC under current and future climates.

Materials and Methods

Study site

All research was done at the Puéchabon experimental site, located on a flat plateau at 35 km northwest of Montpellier (southern France; 43°44′29″N, 3°35′45″E, 270 m above sea level). The site is situated in a Mediterranean forest, with *Q. ilex* L. as the dominant tree species. The forest has been managed as a coppice for centuries, and the last clear cut was performed in 1942. In 2016, the top canopy height was 5.5 m on average and the stem density of *Q. ilex* was 4544 (± 719) stems-ha^{-1}. The climate is Mediterranean with a mean annual precipitation of 953 mm and a mean annual temperature of 13.5°C (on average; 1989–2018). A shallow bedrock and a high volumetric fractional content of stones (0.75 for the top 0–50 cm and 0.90 below) impose a strong constraint on water availability.
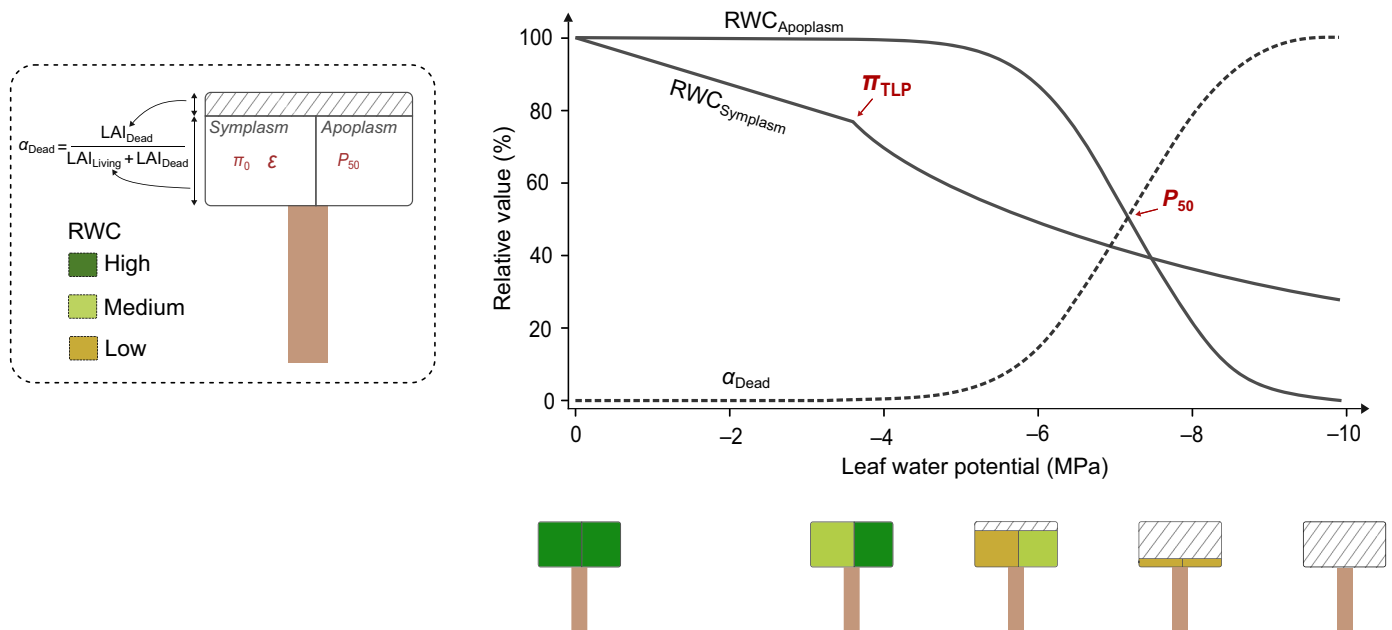
Fig. 1 Schematic representation of the processes and traits involved in the dynamics of canopy fuel moisture content (CFMC) and live fuel moisture content (LFMC) in the plant-hydraulic model *SurEau-Ecos-FMC*. Canopy fuel moisture content is defined as the weighting sum of the water content (per dry mass) of the LFMC and dead fuel moisture content (DFMC) shoots. The ratio of dead-to-live fuel in the canopy (α_{Dead}) determines the proportion of dead leaves in the canopy and is a function of percent loss of conductance in the leaves (PLC$_{Leaf}$, %). α_{Dead} is a function of the leaf area index of dead and live foliage (LAI$_{dead}$ and LAI$_{Live}$, respectively). P_{50} (MPa) is the water potential causing 50% loss of plant-hydraulic conductance. The response of LFMC to leaf water potential (ψ_{Leaf}, MPa) is obtained by a model based on pressure–volume (p-v) curves that describe the dynamics of water content in two distinct compartments: the relative water content of the symplasmic compartment (RWC$_{Sym}$, living cells) and the relative water content of the apoplasmic compartment (RWC$_{Apo}$, extracellular xylem water). The shape of p-v curves mainly depends on the osmotic potential at full turgor (π_0, MPa) and the elasticity of cell walls (ε, % MPa^{-1}). π_{TLP} (MPa) is the turgor loss point derived from p-v curves. Dead fuel moisture content is assumed to be disconnected from the plant-hydraulic pathway and follows the variations of the vapor pressure deficit of the air.

Datasets

Canopy and leaf measurements Different measurements were conducted for the period from 2016 to 2018. Leaf water potential (ψ_{Leaf}) and LFMC were measured at predawn and at midday for five trees during the summer drought of each year (May to October) approximately once every 3 wk. At each date, two or three leafy shoots per tree were sampled from the upper part of the canopy, rapidly sealed in a plastic bag, and stored in a cooler, according to Rodriguez-Dominguez *et al.* (2022). ψ_{Leaf} was measured within 2 h using a Scholander pressure bomb (PMS1000; Corvallis, OR, USA). Three to six leaves were collected concomitantly from the same trees for LFMC measurements, stored in sealed plastic bags upon collection, and stored in a cooler. At the laboratory, leaf samples were weighted fresh and then dried in an oven at 60°C for 48 h and weighted again to compute LFMC. *Quercus ilex* bud burst generally occurs in April, and the new shoots expand and maturate until early July (Limousin *et al.*, 2012). To avoid any bias in LFMC estimations that might arise from phenological differences between leaves, measurements were always made on mature leaves. As a proxy of foliage mortality, we derived an estimation of foliage mortality from continuous measurements of the Normalized Difference Vegetation Index (NDVI) made using a sensor positioned above the canopy. For each year, we estimated the foliage change during the summer drought period as the relative variation in NDVI between

leaf maturity (around early July) and the end of the summer. We also measured tree transpiration on six trees with stem sap flow sensors recording data since 2004 (see Gavinet *et al.*, 2019).

Meteorological data Meteorological data (precipitation, temperature, relative humidity, global radiation, and wind speed) used as input in *SurEau-Ecos-FMC* were collected by a weather station located in a clearing < 100 m away from the experimental site.

Climate variables for the future period (2005–2100) used as input in projections were obtained from the climate simulation program involved in the fifth phase of the Coupled Model Intercomparison Project and produced as part of the EURO-CORDEX initiative (Kotlarski *et al.*, 2014). Thirteen GCM–RCM couples were selected and extracted at a 0.44° spatial resolution for the historical (1990–2005) and future (2006–2099) periods under the RCP4.5 and RCP8.5 scenarios. Model outputs were bias-corrected by a multivariate correction approach (MBCn; Cannon, 2018) using the SAFRAN climate reanalysis database (Vidal *et al.*, 2010) as a reference.

Fuel moisture content modelling

Description of *SurEau-Ecos* *SurEau-Ecos* is a plant-hydraulic model that simulates plant water status and water fluxes between the soil, plant, and the atmosphere for a mono-specific layer of vegetation (Ruffault *et al.*, 2022). It predicts, at an hourly time

step, water potentials and water content of the plant and soil as a function of soil properties, plant-hydraulic traits, stand structure, and daily climatic variables. *SurEau-Ecos* draws on the equations and mechanisms developed in the *SurEau* model (Martin-StPaul *et al.*, 2017; Cochard *et al.*, 2021), and on the SIERRA water balance model (Mouillot *et al.*, 2001; Ruffault *et al.*, 2013). In *SurEau-Ecos*, the soil–plant system is discretized into two plants organs (a 'Leaf' and a 'Stem') and three soil layers. Each plant organ consists of an apoplasmic and a symplasmic compartment (Tyree & Yang, 1990), whose capacitances are simulated by different physiological mechanisms. Symplasmic capacitances are derived from *p-v* curves (Tyree & Hammel, 1972) and apoplasmic capacitances from vulnerability curves to cavitation (Cruiziat *et al.*, 2002). Soil layers are characterized by variations of soil-to-root conductance. Soil water potential in the rhizosphere depends on the normalized water content and is calculated with the van Genuchten–Mualem equations (van Genuchten, 1980). Main stand parameters are the LAI ($m^2_{leaf} \times m^{-2}_{soil}$), which set the amount of water losses from the ecosystem and the stem volume ($m^3 \times m^{-2}_{soil}$) that includes the volume of the root, trunk, and branches. Stomatal response to light and temperature is modelled following Jarvis (1976).

SurEau-Ecos-FMC   We implemented a new FMC module into *SurEau-Ecos* to simulate FMC dynamics of fine canopy fuels (shoot and leaves) at the leaf and canopy levels. Live fuel moisture content usually represents the moisture content of live fine fuel at the leaf level. We also introduced the CFMC, to represent the moisture content of fine fuel (live and dead) at the canopy level and integrate the impact of foliage mortality that can occur under drought.

This *SurEau-Ecos-FMC* model relies on two main mechanisms. The relationship between leaf water potential leaf (ψ_{Leaf}) and its relative water content (RWC) is computed from *p-v* curves (Tyree & Hammel, 1972). The percent loss of leaf hydraulic conductance due to embolism (PLC$_{Leaf}$) is derived from ψ_{Leaf} through vulnerability curves to cavitation and affects the dynamics of FMC in two different ways. At the leaf level, PLC$_{Leaf}$ dictates the dynamics of the leaf apoplasmic reservoir. At the canopy level, it drives the proportion of dead fuel within the canopy (α_{Dead}). Dead leaves are assumed to remain on the tree but are disconnected from the tree hydraulic pathway, thereby lowering transpiration and mitigating the impact of drought by the reduction in the LAI. Leaf embolism is not reversible during the vegetation season. A list of the input parameters of *SurEau-Ecos-FMC* can be found in Supporting Information Table S1.

Fuel moisture content (in % of dry mass) is defined as:

$$\text{FMC} = \frac{F_W - D_W}{D_W} 100 \qquad \text{Eqn 1}$$

where F_W and D_W are the fresh and dry weight (g), respectively.

The CFMC (in % dry mass) follows the weighting sum of the water content of the living and dead leaves such as:

$$\text{CFMC} = \alpha_{dead}\text{DFMC} + (1 - \alpha_{Dead})\text{LFMC} \qquad \text{Eqn 2}$$

where α_{Dead} is the ratio of dead-to-live fuels (vary from 0 to 1), LFMC (% dry mass) and DFMC (% dry mass) are the moisture content of live and dead leaves, respectively. With this approach, CFMC is equal to LFMC in the absence of dead foliage ($\alpha_{Dead} = 0$) and to DFMC when plant foliage is totally dead ($\alpha_{Dead} = 1$). α_{Dead} can be defined as:

$$\alpha_{Dead} = \frac{\text{LAI}_{Dead}}{\text{LAI}_{Dead} + \text{LAI}_{Live}} \qquad \text{Eqn 3}$$

where LAI$_{Dead}$ and LAI$_{Live}$ are the leaf area index of dead and live foliage, respectively, and are defined such as:

$$\text{LAI} = \text{LAI}_{Dead} + \text{LAI}_{Live} \qquad \text{Eqn 4}$$

SurEau-Ecos explicitly accounts for the capacitance related to different reservoirs: the symplasm and apoplasm. Symplasmic capacitances mostly buffer water fluxes during well-watered conditions, while apoplasm capacitances come into play when cavitation occurs, during extreme drought. Following this representation of leaf water reservoirs in *SurEau-Ecos*, LFMC (% dry mass) is defined as the sum of the moisture content in the symplasmic and the apoplasmic compartments weighted by their respective volumetric fraction:

$$\begin{aligned}\text{LFMC} &= \text{LFMC}_{sat}\text{RWC}_{Live} \\ &= \text{LFMC}_{sat}\left[a_f\text{RWC}_{Apo} + (1 - a_f)\text{RWC}_{Sym}\right]\end{aligned} \qquad \text{Eqn 5}$$

where a_f, the fraction of the apoplasmic tissue in the shoots, is an input parameter. LFMC$_{sat}$ (% dry mass) is the fine FMC at water saturation, RWC$_{Apo}$ is the relative water content of the apoplasm, and RWC$_{Sym}$ is the relative water content of the symplasm. Live fuel moisture content is considered as being homogeneous within the canopy, that is potential differences between the LFMC at different heights are not taken into account.

LFMC$_{sat}$ is determined as a function of leaf dry matter content (LDMC; the ratio of leaf dry mass to fresh mass), an input parameter that is widely used as an indicator of plant resource strategies in plant trait databases (e.g. Garnier *et al.*, 2001):

$$\text{LFMC}_{sat} = \frac{1}{\text{LDMC}} - 1 \qquad \text{Eqn 6}$$

RWC$_{Sym}$ and RWC$_{Apo}$ are determined from the water potential of leaf symplasm ($\psi_{Leaf,Sym}$) and water potential of the leaf apoplasm ($\psi_{Leaf,Apo}$), respectively, according to compartment-specific formulations detailed below. $\psi_{Leaf,Sym}$ and $\psi_{Leaf,Apo}$ are both state variables in *SurEau-Ecos*, determined by solving the water balance of each plant compartment (see Ruffault *et al.*, 2022).

RWC$_{Sym}$ is derived from *p-v* curves, which formalize the relationship between RWC$_{Sym}$ and $\psi_{Leaf,Sym}$. The shape of *p-v* curves depends on two main parameters: the osmotic potential at full turgor (π_0, MPa) and the elasticity of cell walls (ε, % MPa^{-1}). Both parameters can be derived from laboratory measurement datasets and are currently available for many species (Bartlett

et al., 2012; Martin-StPaul *et al.*, 2017). RWC_{Sym} is calculated using the following equation depending on whether $\psi_{Leaf,Sym}$ is below or above the turgor loss point (π_{TLP}), which is derived from *p-v* curves (Bartlett *et al.*, 2012):

$$RWC_{Sym} = \begin{cases} \min\left(\dfrac{-\left(\psi_{Leaf,Sym} + \pi_0 - \varepsilon\right) \pm \sqrt{\left(\psi_{Leaf,Sym} + \pi_0 - \varepsilon\right)^2 - 4\varepsilon\psi_{Leaf,Sym}}}{2\varepsilon} \right), \psi_{Leaf,Sym} > \pi_{TLP} \\ \\ 1 - \left(1 - \dfrac{\pi_0}{\pi_{TLP}}\right), \psi_{Leaf,Sym} \le \pi_{TLP} \end{cases} \quad \text{Eqn 7}$$

RWC_{Apo} decreases proportionately with the rate of embolism in the leaves. This process is not reversible during the vegetation season:

$$RWC_{Apo} = 1 - \frac{PLC_{Leaf}}{100} \quad \text{Eqn 8}$$

where PLC_{Leaf} (%) is the percent loss of conductance in the leaves and is determined as a function of ψ_{LApo} such as:

$$PLC_{Leaf} = \frac{100}{1 + e^{\left(\frac{slope_L}{25} \cdot \left(\psi_{LApo} - P_{50,L}\right)\right)}} \quad \text{Eqn 9}$$

where $P_{50,L}$ (MPa) is the water potential causing 50% loss of plant-hydraulic conductance, and $slope_L$ (% MPa^{-1}) is the slope of linear rate of embolism spread per unit water potential drop at the inflection point $P_{50,L}$.

The ratio of dead-to-live fuels (α_{Dead}) increases proportionately with PLC_{Leaf} such as:

$$\alpha_{Dead} = \begin{cases} 0, & PLC_{Leaf} \le 10\% \\ PLC_{Leaf}, & PLC_{Leaf} > 10\% \end{cases} \quad \text{Eqn 10}$$

Finally, FMC_{Dead} follows the atmospheric vapor pressure deficit (VPD, kPa) according to an exponential decline function (Resco de Dios *et al.*, 2015):

$$DFMC = FM_0 + FM_1 \times e^{-mVPD} \quad \text{Eqn 11}$$

where FM_0 is the minimum measured fuel moisture, $FM_0 + FM_1$ is the maximum measured fuel moisture, and *m* defines the rate of moisture decay with increasing VPD. FM0, FM1, and *m* are all input parameters in *SurEau-Ecos-FMC*.

Model parametrization The default parametrization of *SurEau-Ecos-FMC* for *Q. ilex* at the Puéchabon site was based on a review of the existing literature on the site. The full list of parameters and how they were estimated, either from previous studies or from specific methodologies (in the case of parameters that were not directly available), is summarized in Table S1.

Leaf area index was set to 2.2, a value slightly lower than in previous publications but in agreement with the recent decrease following severe droughts in 2016 and 2017. The thickness of the three soil layers and their rock fragment content were defined according to stone content measurements in the field and to match the estimated rooting depth (> 4.5 m; Rambal *et al.*, 2003). The parameters of the van Genuchten (1980) water retention curve were adjusted so as to reduce the bias between observed and simulated predawn water potential while remaining within the range of the *in situ* estimation of the total available water (TAW) capacity based on eddy-covariance data (i.e. 139 mm). The resulting TAW content cumulated over the three soil layers was 125 mm when considering the difference between the water quantity at field capacity and the water quantity at leaf P_{50} (−6.4 MPa). This is slightly lower than previously published values (De Cáceres *et al.*, 2021) but in agreement with transpiration estimations from sap flow measurements used in this study (Gavinet *et al.*, 2019).

The total hydraulic conductance per unit leaf area was computed using sap flow measurements and water potential gradients (between predawn and midday; Gavinet *et al.*, 2019) and distributed in the plant assuming that 40% of the resistance was located between the leaf apoplasm and the leaf symplasm and the remaining 60% between the roots and the leaf apoplasm. Root distribution within the soil was set to the value reported by Jackson *et al.* (1996) for the Mediterranean biome. The proportion of resistance attributed to the roots in each soil layer (i.e. one root per soil layer) was considered to be equal to the relative proportion of root length in each soil layer.

The water potential causing 50% stomatal closure (ψ_{gs50}) was set at −1.85 MPa, as determined by concurrent measurements of leaf gas exchanges and ψ_{Leaf} by Limousin *et al.* (2010). Minimum leaf conductance ($g_{cuti,20}$) determines the residual water loss after stomata are closed and was taken from Limousin *et al.* (2022). The dependence of the minimum leaf conductance to temperature was simulated through two Q_{10} functions (Cochard, 2021) whose parameters were taken from measurements reported in Billon *et al.* (2020).

Leaf traits including leaf mass per area, succulence, and *p-v* curve parameters (π_0, ε) were taken from Limousin *et al.* (2022). Pressure–volume curve parameters were set equal for the leaf and stem symplasms assuming no hydraulic segmentation of these traits within the different organs of the plant. The parameters of the vulnerability curves to cavitation for the stem were derived

from Sergent *et al.* (2020). For the leaf, parameters were derived from vulnerability curves measurements performed in early 2019 on the same six trees on which ψ_{Leaf} and LFMC were monitored. Leaf vulnerability to cavitation was assessed using the optical technique (Brodribb *et al.*, 2016) and the protocol by Lamarque *et al.* (2018).

Model evaluation Our evaluation of *SurEau-Ecos-FMC* consisted of four different phases. First, we compared simulated and measured ψ_{pd}, ψ_{md}, and transpiration fluxes. Then, we evaluated the ability of *SurEau-Ecos-FMC* to simulate LFMC from ψ_{Leaf} (Eqns 5–8). Three sets of model parameters were tested: (1) parameters derived from on-site measurements (described under Canopy and leaf measurements in the Materials and Methods section), and parameters derived from a procedure that aimed to optimize the fit between observed and measured LFMC either (2) on the whole dataset, or (3) for each year independently. This last option allowed a potential yearly plasticity of hydraulic traits (particularly π_0) to be taken into account. Only the *p-v* curve parameters (π_0, ε, and LDMC), known to change according to drought (Bartlett *et al.*, 2012), were adjusted here. Parameters of the vulnerability curve to cavitation were set constant (described under Canopy and leaf measurements in the Materials and Methods section) as it is expected to exhibit little changes in response to drought variations (Limousin *et al.*, 2010, 2022; Martin-Stpaul *et al.*, 2013). In a third step, we compared simulated and measured at predawn and at midday LFMC. Finally, we compared foliage mortality (α_{Dead}) estimated by *SurEau-Ecos-FMC* with measured NDVI variations. For these two last steps, we used *p-v* curve parameters resulting from the optimization over the 3-yr period.

Model sensitivity to species traits and stand parameters In order to gain insight into the influence of hydraulic traits and stand parameters in the dynamics of FMC, we carried out a variance-based sensitivity analysis. We used the Sobol' sensitivity analysis method (Sobol, 2001) and reported 'total order indices' that quantify the contribution of each parameter to the variance of the model output. For each parameter, we randomly sampled a value within a range of $\pm$ 20% of the observed value. Starting from a wet soil, we ran simulations with the same climate input and reported for each simulation the minimum leaf and canopy moisture content reached during the simulation (LFMC$_{\text{min}}$ and CFMC$_{\text{min}}$).

The selection of parameters was based on previous sensitivity analyses performed on *SurEau* (Cochard *et al.*, 2021) and *SurEau-Ecos* (Ruffault *et al.*, 2022) as well as from the results of preliminary analyses. We focused on LAI$_{\text{max}}$, TAW, P$_{50}$, $g_{\text{cuti,20}}$, ε, π_0, Q_{10a}, T_P, ψ_{gs50}, and α_f (Table 1). Total available water is not an input parameter in *SurEau-Ecos-FMC* but can be computed as an integrative index resulting from the interaction between soil characteristics and rooting depth (see Model parametrization in the Materials and Methods section). To make TAW vary in simulations without affecting soil physical properties, we modified rooting depth such as to match the targeted TAW. To ease the interpretation of the results of the sensitivity analyses, all traits were grouped in three different traits families:

Table 1 List of the main traits influencing the dynamics of fuel moisture content (FMC) at the Puéchabon *Quercus ilex* forest in *SurEau-Ecos-FMC* and selected for the global sensitivity analyses.

Family	Symbol	Variable	Unit	Value
Water use and regulation	LAI$_{\text{max}}$	Maximum leaf area index	–	2.2
	TAW*	Total available water capacity for the plant	mm	145
	ψ_{gs50}	Water potential causing 50% stomatal closure	MPa	1.85
	$g_{\text{cuti,20}}$	Cuticular conductance at 20°C	mmol m^2 s^{-1}	3
	Q_{10a}	Temperature dependence of g_{cuti} when $T \leq T_{\text{Phase}}$	–	1.2
Vulnerability to cavitation	P_{50}	Water potential causing 50% loss of leaf hydraulic conductance	MPa	−7
p-v curves	ε	Leaf modulus of elasticity	MPa	15
	π_0	Osmotic potential at full turgor	MPa	−2.5
	α_f	Apoplasmic fraction	–	0.4

Traits were grouped into three different families: water use and regulation, vulnerability to cavitation, and *p-v* curve. All traits varied from $\pm$ 20% around their original value. *,TAW is not an input parameter in *SurEau-Ecos-FMC* but an integrative value of soil characteristics and rooting depth. The list of all parameters is provided in Table S1.

'water use and regulation' (LAI$_{\text{max}}$, TAW, ψ_{gs50}, g_{cuti}, and Q_{10a}), 'vulnerability to cavitation' (P_{50}), and '*p-v* curves' (ε, π_0, and α_f).

Projections of fuel moisture content. To explore tree sensitivity to future climate change, we projected FMC for the period 1985–2100 using an ensemble of 13 GMC-RCM couples for two emission scenarios (described under Canopy and leaf measurements in the Materials and Methods section) as climate inputs. To assess the potential impact of tree adaptation to a drier climate, two sets of projections were simulated. In the first set, we used the same parameterization used for model evaluation (described under Model parametrization in the Materials and Methods section; Table S1). In the second set, LAI was reduced by 20%, following the response of the *Q. ilex* forest to a throughfall exclusion experiment that reduced the precipitation input to the soil by 29% (Limousin *et al.*, 2009). For each simulation, stand parameters were re-initialized each year assuming that the stand remained identical in terms of species and structure.

Results

Comparisons between simulated and measured leaf water potentials

SurEau-Ecos-FMC captured the decrease in predawn and midday ψ_{Leaf} well during the summer drought and their recovery
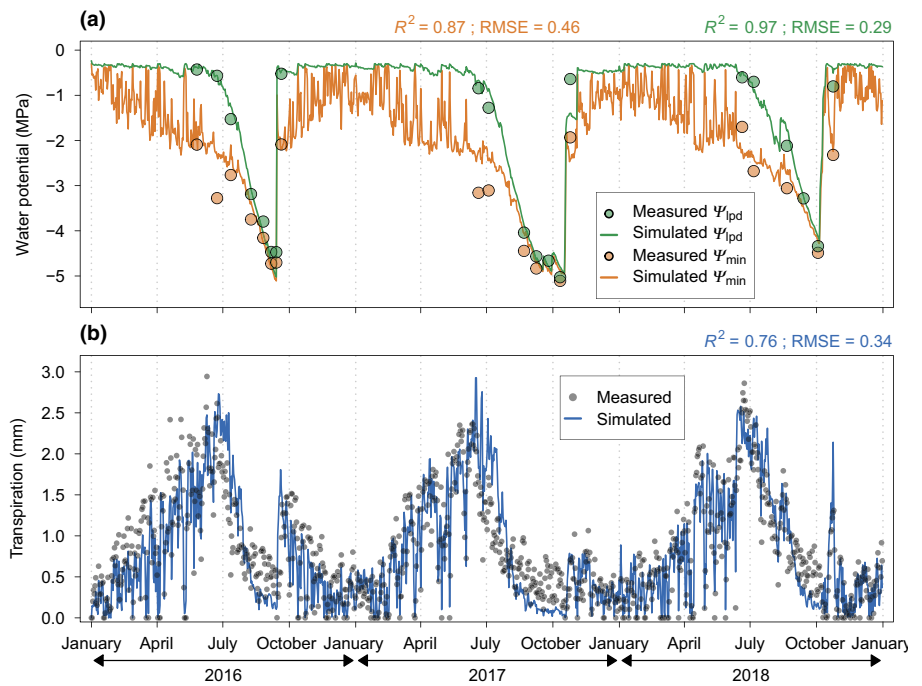
Fig. 2 Comparison between simulated and observed (a) leaf water potential and (b) canopy transpiration in a *Quercus ilex* stand at the Puéchabon study site over a 3-yr period (2016–2018). Leaf water potential and transpiration were simulated with the plant-hydraulic model *SurEau-Ecos*. At each date, values of predawn (ψ_{pd}) and midday (ψ_{min}) leaf water potentials are shown.

Fig. 3 Measured and simulated relationships between leaf live fuel moisture content (LFMC, % dry mass) and leaf water potential (ψ_{Leaf}, MPa) over a 3-yr period (2016–2018) in a *Quercus ilex* stand at the Puéchabon study site. Measurements at predawn and midday are shown. Live fuel moisture content was estimated from leaf water potential with *SurEau-Ecos-FMC* by using either (a) measured parameters, (b) optimized parameters, or (c) an optimized parameter independently for each year. RMSE and R^2 are indicated.
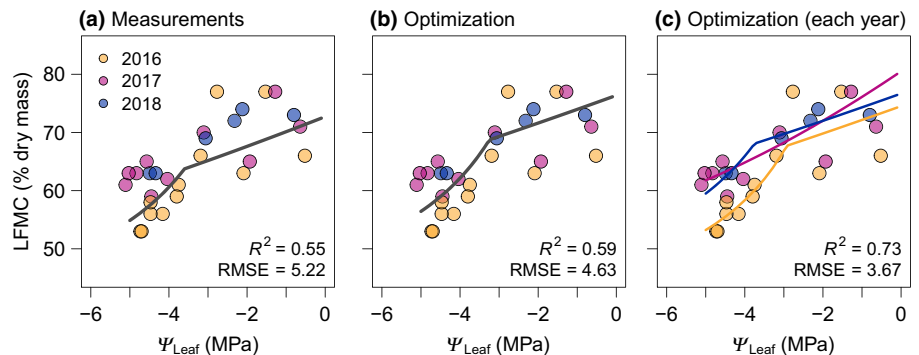
(Fig. 2a). The model explained 98% and 87% of the variance in ψ_{pd} and ψ_{md}, respectively. The model also predicted the dynamics of stand transpiration fluxes well ($R^2 = 0.76$, RMSE = 0.34 mm).

Leaf-level fuel moisture content dynamics in relation to plant water potential

Overall, LFMC estimated from ψ_{Leaf} through *p-v* curves (Eqns 5–8) was in satisfactory agreement with LFMC measurements (Fig. 3). When using measured parameters as input in *p-v* curves, we explained 55% of the variance in measured LFMC with only little biases (RMSE = 5.2%). Similar results were obtained when using optimized parameters ($R^2 = 0.59$, RMSE = 4.63%). However, we noticed that both models (measured and optimized parameters) diverged from measurements for the lowest values of ψ_{Leaf}. Using optimized parameters for each year lowered this bias while improving the overall predictability of LFMC ($R^2 = 0.73$; RMSE = 3.7%).

Comparisons between simulated and observed LFMC

Temporal dynamics of LFMC measured at the Puéchabon site was well predicted by the model over the three studied years (Fig. 4a), explaining 69% (RMSE = 4.27%) and 74% (RMSE = 4.92%) of the variance in $LFMC_{pd}$ and $LFMC_{md}$, respectively. When drought conditions were not that intense, most of the decrease in LFMC was due to a symplasmic water decrease while, under severe drought, an apoplasmic decline due to drought-induced embolism was observed (Fig. 4b). As the apoplasmic compartment does not recover in our simulations, this effect lasted beyond the dry period.

Simulations of canopy fuel moisture content

Our simulations predicted a rate of leaf embolism of *c.* 20% during the summers of 2016 and 2017 (Fig. 5a). Foliage mortality induced by leaf embolism led to a decrease in CFMC compared
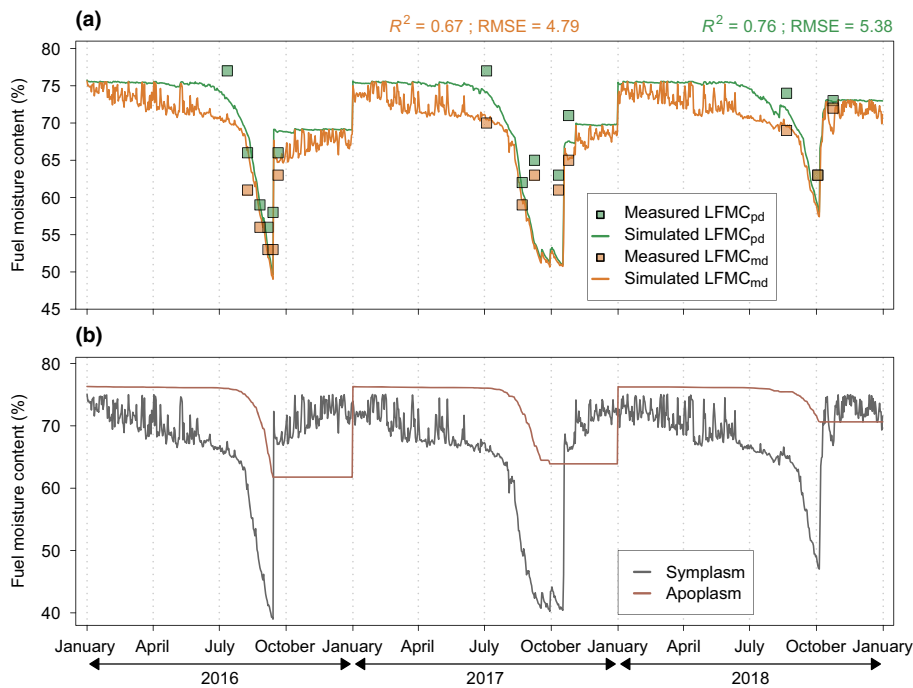
Fig. 4 Comparison between observed and simulated live fuel moisture content (LFMC) by the plant hydraulic model *SurEau-Ecos-FMC* in a *Quercus ilex* stand at the Puéchabon study site over a 3-yr period (2016–2018). (a) Observed and simulated values of LFMC at predawn (LFMC$_{pd}$) and midday (LFMC$_{md}$). (b) Simulated dynamics of the symplasmic and apoplasmic leaf moisture content.
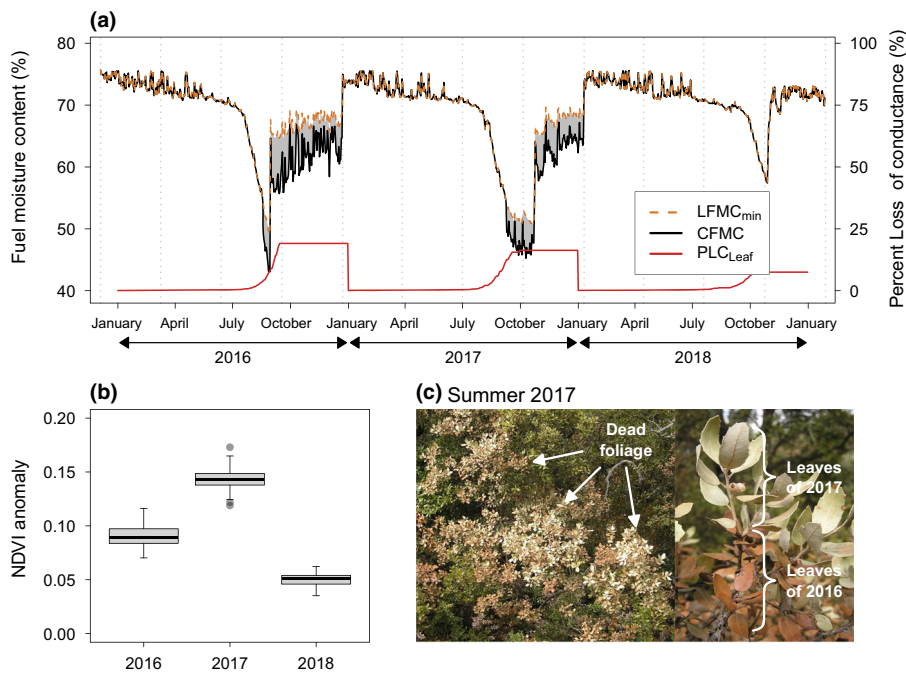

Fig. 5 Comparison between simulated canopy fuel moisture content (CFMC) by the plant-hydraulic model *SurEau-Ecos-FMC* and indicators of foliage mortality in a *Quercus ilex* stand at the Puéchabon site over a 3-yr period (2016–2018). (a) Simulated dynamics of daily minimum LFMC (LFMC$_{md}$), daily minimum CFMC (CFMC$_{md}$), and leaf percent loss of conductance (PLC$_{Leaf}$). Leaf area index and plant-hydraulic conductances were reset to their initial value every year. (b) Standardized variations between NDVI measured at leaf maturity (early July) and at the end of summer drought (mid-October). (c) Picture showing the leaf desiccation that occurred at the end of the 2017 summer at the Puéchabon site.

with LFMC. These results are consistent with a higher relative change in NDVI during 2016 and 2017 than in 2018 (Fig. 5b). However, our model was not able to discriminate the level of CFMC between the years 2016 and 2017 (Fig. 5c).

Sensitivity analyses

A few species-specific and stand traits explained most of the variability in the yearly minimum canopy moisture content

(CFMC$_{min}$) and yearly minimum LFMC (LFMC$_{min}$; Fig. 6). Traits related to 'water use and regulation', namely LAI$_{max}$, TAW and ψ_{gs50}, had the highest contribution to the variations of both CFMC$_{min}$ and LFMC$_{min}$. As expected, lower levels of fuel moisture were associated with parameter values that either minimize water losses (higher LAI$_{max}$) or increase water reserves (lower TAW; Fig. 6). Then, 'hydraulic safety' traits (P_{50}) mostly drove the variations in CFMC$_{min}$, while 'plant water storage traits', namely π_0, had the greatest influence on LFMC$_{min}$.
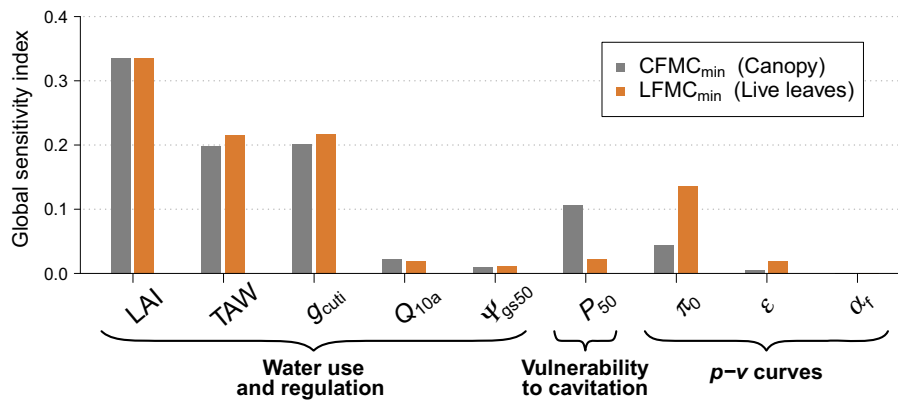
Fig. 6 Global sensitivity analysis of live fuel moisture content (LFMC) and canopy fuel moisture content (CFMC) to species and stand traits for *Quercus ilex* in the plant-hydraulic model *SurEau-Ecos-FMC*. $LFMC_{min}$ is the minimum LFMC reached during the year and $CFMC_{min}$ is the minimum CFMC reached during the year. All traits varied from $\pm$ 20% around their original value; LAI, leaf area index; TAW, total available water capacity for the plant; ψ_{gs50}, water potential causing 50% stomatal closure; g_{cuti}. cuticular conductance at 20°C, Q_{10a}, temperature dependence of g_{cuti}; P_{50}, water potential causing 50% loss of leaf hydraulic conductance; ε, leaf modulus of elasticity; π_0, osmotic potential at full turgor; α_f, apoplasmic fraction.

Projections of fuel moisture content

Our projections predicted a general decrease in FMC over the next century but with major differences between emission scenarios and according to whether or not drought adaptation (LAI reduction) was accounted for (Fig. 7). When no adaptation was simulated, both $LFMC_{min}$ and $CFMC_{min}$ but with higher magnitudes of change for $CFMC_{min}$. $CFMC_{min}$ would decrease from an average value of 64.6% under current climate (1985–2015) to 58.4% and 41.1% for the end of the century (2071–2099) under RCP4.5 and RCP.85, respectively. A large part of this decline was due to foliage mortality as PLC_{Leaf} was predicted to increase from 3.4% under current climate up to 28.9% for the end of the century under RCP8.5 (Fig. 7e). Reducing the LAI by 20% significantly contributed to reduce the predicted impact of climate change on FMC. It would almost fully compensate the effects of climate change under RCP4.5 but not under RCP8.5 where $CFMC_{min}$ would still decrease to 55.8% by the end of the century (Fig. 7b).

Discussion

While the literature is rich in mechanistic models that simulate plant water potential, much less attention has focused on the prediction of FMC. Here, we developed *SurEau-Ecos-FMC*, a plant-hydraulic model predicting both LFMC and CFMC. We discuss in more detail below the strengths and limits of our framework as well as the implications of our results for the understanding and prediction of wildfire danger in a changing climate.

Fuel moisture sensitivity to climate is explained by species and stand traits

Our physiological approach of FMC highlights that the plant moisture sensitivity to climate can be explained by a few species-specific and stand traits that drive the plant exposure to drought on the one hand, and the level of dehydration for a given

exposure on the other. Plant exposure to drought is primarily controlled by a set of traits that define the plant 'water use and regulation', including in particular the LAI, TAW, and stomatal regulation (ψ_{gs50}). Leaf area index and ψ_{gs50} drive the water demand during drought and TAW the water supply. Taken together, they explain the response of leaf water potential (ψ_{Leaf}) to given climate conditions and therefore determine, to a large part, both LFMC and CFMC dynamics. Accordingly, the reduction in tree transpiration through adjustment of the leaf area was found to significantly reduce the projected impact of future climate change at our study site. As for the traits driving the level of dehydration for a given exposure, they depend upon the scale under consideration. At the leaf level, traits related to the variation symplasmic water stores during drought (*p-v* curve traits), and in particular the osmotic potential at full turgor (π_0), significantly influenced LFMC variations, as already suggested by Nolan *et al.* (2018). At the canopy level, the hydraulic safety traits related to the vulnerability to xylem embolism (summarized here by the water potential causing 50% loss of leaf hydraulic conductance; P_{50}) were the most influential parameters. This mirrors the proportionality between the embolism rate and foliage mortality implemented into the model (Eqn 10), an assumption based on the results of several studies that demonstrated the link between canopy damage and leaf hydraulic failure (Hammond *et al.*, 2019; Cardoso *et al.*, 2020; Klein *et al.*, 2022).

Drivers of leaf-level moisture content: *p-v* curves and osmotic processes

Our approach to predict LFMC relied on different physiological mechanisms that drive the dynamics of plant desiccation during drought: *p-v* curves for the symplasm and leaf xylem vulnerability to cavitation for the apoplasm (Eqns 5–8; Fig. 1). *SurEau-Ecos-FMC* therefore builds on the theoretical framework from Nolan *et al.* (2018) while extending it to include embolism affecting leaf tissues under extreme drought. Accordingly, most of the leaf-level LFMC variations were attributable to the symplasm
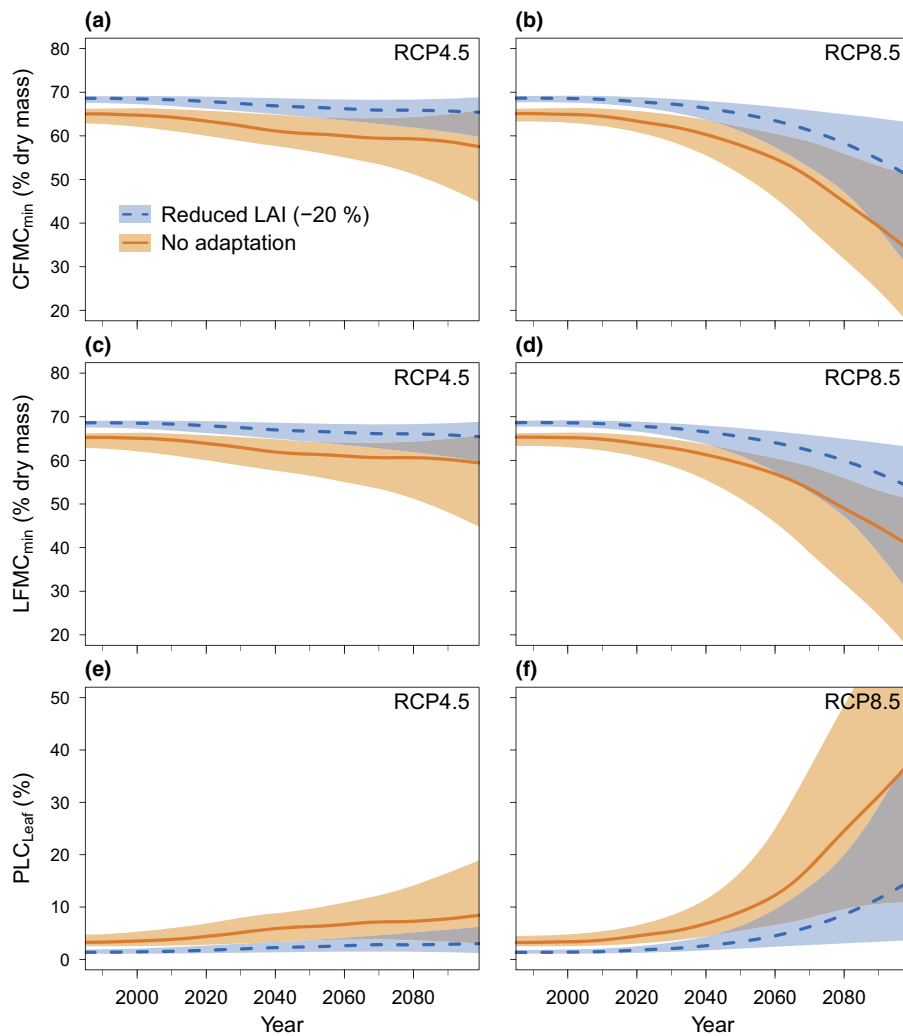
Fig. 7 Multimodel mean changes in fuel moisture content (FMC) in a *Quercus ilex* stand at the Puéchabon study site simulated with the plant-hydraulic model *SurEau-Ecos-FMC* over the period 1985–2099. Means across climate models (lines) and uncertainty (shaded areas; 5th and 95th quantiles) are shown for two emission scenarios (RCP4.5 and RCP8.5) under two sets of simulations: one where traits were fixed to their current value and one where leaf area index (LAI) was reduced by 20%. LFMC$_{min}$, minimum LFMC reached during the year (panels a, b); CFMC$_{min}$, minimum CFMC reached during the year (panels c, d); PLC$_{Leaf}$, leaf percent loss of conductivity (panels e, f).

response to ψ_{Leaf} (Fig. 4b). By contrast, the apoplasmic compartment which represents a smaller proportion of the water in leaves and emptied only under intense drought when embolism occurred had a lower role in leaf-level LFMC variations, as evidenced by our sensitivity analyses.

Our work therefore provides further evidence that *p-v* curves are a relevant framework for LFMC predictions (Nolan *et al.*, 2018; Pivovaroff *et al.*, 2019; Scarff *et al.*, 2021). When using measured trait values, the predictability of LFMC from measured ψ_{Leaf} was relatively high ($R^2 = 0.55$, Fig. 3). However, our study further showed that LFMC predictions were significantly improved when assuming year-to-year changes in the value of π_0 (i.e. osmotic adjustment; Fig. 3). Osmotic adjustment, a biochemical process that maintains tissue hydration and turgor when water potential decreases, has been identified as an acclimation mechanism for many tree species (Bartlett *et al.*, 2014) including *Q. ilex* (Limousin *et al.*, 2022). The integration of osmotic adjustments in plant-hydraulics model has, so far, received limited attention (but see Rieger, 1995) and therefore presents a path for improving our understanding of LFMC sensitivity to climate.

One important assumption of our study was to consider the maximum level of moisture content of the leaves (LFMC$_{sat}$; Eqn 6) as a constant value throughout the simulations. This hypothesis is valid for a specific forest stand at the scale of a summer drought when leaf growth is limited, and LFMC variations are driven more by the variations in the water content of the leaves than in their dry matter. However, at broader spatial and temporal scales, several studies showed that the variations in LDMC can have a much more important role in the variations of LFMC (Jolly *et al.*, 2014, 2016; Jolly & Johnson, 2018; Brown *et al.*, 2022; Nolan *et al.*, 2022). The integration of phenological and adaptative processes affecting dry mass dynamics into process-based models is therefore an important but challenging step toward improving fuel moisture predictions over broader spatial and temporal scales.

Foliage mortality is the main driver of canopy fuel moisture content

The main objective of our study was to move forward from LFMC (leaf-level) to CFMC (canopy-level) modelling by taking

into account foliage mortality that can occur under extreme drought (Klein *et al.*, 2022). Not surprisingly, we found that the influence of the dead-to-live fuel ratio (α_{Dead}) in CFMC variability increases with increasing drought. At the Puéchabon site, foliage mortality in *SurEau-Ecos-FMC* reached almost 20% during the summers of 2016 and 2017, in accordance with NDVI declines (Fig. 5b) and *in situ* observations of leaf browning at the site (Fig. 5c). Our projections further showed that the impact of foliage mortality on CFMC dynamics is expected to increase in importance as climate continues to warm (Fig. 7).

The impact of partial canopy mortality on CFMC has been discussed by several authors (Jolly & Johnson, 2018; Karavani *et al.*, 2018; Nolan *et al.*, 2020a) but not fully integrated within a modelling framework. Here, we proposed a semimechanistic prediction of foliage mortality, integrating recent knowledge on plant hydraulics by simulating α_{Dead} as a function of leaf embolism (Fig. 1a). In this approach, however, α_{Dead} was regarded as a global canopy parameter, which means that the distribution of accumulated dead fuel within the canopy is not accounted for. Mortality can take place at the leaf, branch, or tree level and preferentially occur, for instance, in the sun-exposed parts of the canopy than in shaded parts. Current LFMC databases are based on the analysis on living materials and do not report the amount of dead fuel and its distribution within the canopy (Martin-StPaul *et al.*, 2018; Yebra *et al.*, 2019; Gabriel *et al.*, 2021). We therefore encourage the development of more detailed databases that include not only measurements of LFMC over a range of time frames but also the spatial and temporal distribution of dead fuel within forest canopies.

We hypothesized that drought-induced embolism affected CFMC through two complementary mechanisms acting on different plant scales (Fig. 1). At the leaf level, it dictates the dynamics of the leaf apoplasmic reservoir. At the canopy level, it drives the ratio of dead-live fuel (α_{Dead}) within the canopy (Fig. 1). The validity of this hypothesis remains, however, difficult to evaluate. Important knowledge gaps are still there in our understanding of how and where hydraulic damages occur within the plant. Our results on *Q. ilex* showed that including both mechanisms was *a priori* a reasonable assumption to simulate both LFMC and CFMC dynamics (Figs 5, 6), but we cannot draw definite conclusions about the relevancy of this hypothesis from these results only. The development of future works focusing on the response of the different plant organs to decreasing water potentials during drought across tree species with contrasting water use strategies and hydraulic traits (e.g. Cardoso *et al.*, 2020) is a key research avenue to predict future fire disturbances.

Implications for the understanding and prediction of wildfire danger under a changing climate

Unlike standard meteorological-based indices generally used to characterize wildfire danger, LFMC and CFMC integrate the underlying physiological and hydrological mechanisms determining vegetation's sensitivity to drought. According to the recent study by Rao *et al.* (2022), wildfires tend to occur more frequently in regions where FMC of the vegetation shows greater sensitivity to

drought. Thanks to our process-based approach of fuel moisture, we highlighted here the physiological mechanisms driving the sensitivity of FMC to climate, which could be used as a basis to better understand the patterns of FMC across landscapes.

Quantifying future trends and patterns of FMC and identifying their drivers are important tasks, in particular in view of the emergence of global novel extreme wildfire events (Ruffault *et al.*, 2020; Duane *et al.*, 2021). This is, however, confronted with the challenge of investigating complex forest systems that are characterized by long-term dynamics and high uncertainties. Process-based models such as *SurEau-Ecos-FMC* have the potential to provide anticipatory predictions of possible futures according to different ecological hypotheses. Thus, we found that theoretical trajectories without any adaptation would lead to very low CFMC, and while potential adaptive mechanisms (such LAI reduction) can lower these trends, this may not be sufficient to mitigate the effects of climate change under the RCP8.5 emission scenario (Fig. 7). On longer time scales, other changes can occur, such as shifts in species composition that can lead to the emergence of new trait combinations (Guillemot *et al.*, 2022). Coupling *SurEau-Ecos-FMC* with forest dynamics models (Morin *et al.*, 2021) would allow to explore the potential feedbacks between changes in vegetation composition and wildfire danger.

Translating the projected dynamics and trends of future FMC into wildfire danger is, however, not straightforward. In addition to fuel moisture, wildfire behavior depends on many other interacting factors including wind speed, temperature, topography, and the load and distribution of fuel. A promising direction for our understanding of wildfire lies in the coupling between *SurEau-Ecos-FMC* and fire behavior models such as FIRETEC (Linn *et al.*, 2002). Fire behavior models can capture the influence of fuel moisture on fire behavior and therefore evaluate the outcome, in terms of wildfire danger, of many feedbacks between ecosystem functioning and response to drought (Banerjee *et al.*, 2020). Such a coupling between process-based models of fuel moisture and fire behavior models would certainly help to narrow the current gap between plant ecophysiology, forest management, and fire sciences. An important question for future research in that area will be to determine the drivers of the residence times of dead leaves on the trees, that is currently not addressed in our model. Another potential contribution of *SurEau-Ecos-FMC* is to provide regional estimations of vegetation moisture that can help to increase our understanding of how fuel moisture impacts fire regimes, including the spatio-temporal patterns of fire activity, intensity, and severity. The greatest challenges in that will be to parametrize the model at the regional scale and represent the multiplicity of species potentially co-occurring on the same site.

Competing interests

None declared.

Author contributions

JR, NM-S, J-ML, FP, MDC and J-LD designed the research. JR, NM-S and J-ML performed the research. J-ML collected the data at the Puéchabon study site. JR, NM-S, J-ML, FP and J-LD interpreted the results. JR led the writing of the manuscript with inputs from J-ML, FP, J-LD, MDC, HC, FM, CJB, JMT-R, RAP, MM, SD, SJ, AO, BC and NM-S. NM-S developed a preliminary version of the code and wrote a preliminary version of the manuscript.

ORCID

Chris J. Blackman https://orcid.org/0000-0002-7057-956X
Brendan Choat https://orcid.org/0000-0002-9105-640X
Hervé Cochard https://orcid.org/0000-0002-2727-7072
Miquel De Càceres https://orcid.org/0000-0001-7132-2080
Sylvain Delzon https://orcid.org/0000-0003-3442-1711
Jean-Luc Dupuy https://orcid.org/0000-0002-2192-8057
Steven Jansen https://orcid.org/0000-0002-4476-5334
Jean-Marc Limousin https://orcid.org/0000-0003-3701-6973
Nicolas Martin-StPaul https://orcid.org/0000-0001-7574-0108
Myriam Moreno https://orcid.org/0000-0002-6894-2534
Florent Mouillot https://orcid.org/0000-0002-6548-4830
Albert Olioso https://orcid.org/0000-0001-8342-9272
Russell A. Parsons https://orcid.org/0000-0001-5091-8993
François Pimont https://orcid.org/0000-0002-9842-6207
Julien Ruffault https://orcid.org/0000-0003-3647-8172
José M. Torres-Ruiz https://orcid.org/0000-0003-1367-7056

Data availability

Data are available on request from the authors.

References

Abatzoglou JT, Williams AP. 2016. Impact of anthropogenic climate change on wildfire across western US forests. *Proceedings of the National Academy of Sciences, USA* 113: 11770–11775.

Abram NJ, Henley BJ, Sen Gupta A, Lippmann TJR, Clarke H, Dowdy AJ, Sharples JJ, Nolan RH, Zhang T, Wooster MJ *et al.* 2021. Connections of climate change and variability to large and extreme forest fires in southeast Australia. *Communications Earth & Environment* 2: 1–17.

Alizadeh MR, Adamowski J, Nikoo MR, AghaKouchak A, Dennison P, Sadegh M. 2020. A century of observations reveals increasing likelihood of continental-scale compound dry-hot extremes. *Science Advances* 6: aaz4571.

Allen CD, Breshears DD, McDowell NG. 2015. On underestimation of global vulnerability to tree mortality and forest die-off from hotter drought in the Anthropocene. *Ecosphere* 6: art129.

Banerjee T, Heilman W, Goodrick S, Hiers JK, Linn R. 2020. Effects of canopy midstory management and fuel moisture on wildfire behavior. *Scientific Reports* 10: 17312.

Bartlett MK, Scoffoni C, Sack L. 2012. The determinants of leaf turgor loss point and prediction of drought tolerance of species and biomes: a global meta-analysis. *Ecology Letters* 15: 393–405.

Bartlett MK, Zhang Y, Kreidler N, Sun S, Ardy R, Cao K, Sack L. 2014. Global analysis of plasticity in turgor loss point, a key drought tolerance trait. *Ecology Letters* 17: 1580–1590.

Billon LM, Blackman CJ, Cochard H, Badel E, Hitmi A, Cartailler J, Souchal R, Torres-Ruiz JM. 2020. The DroughtBox: a new tool for phenotyping residual branch conductance and its temperature dependence during drought. *Plant, Cell & Environment* 43: 1584–1594.

Brodribb TJ, Skelton RP, Mcadam SAM, Bienaimé D, Lucani CJ, Marmottant P. 2016. Visual quantification of embolism reveals leaf vulnerability to hydraulic failure. *New Phytologist* 209: 1403–1409.

Brown TP, Hoylman ZH, Conrad E, Holden Z, Jencso K, Jolly WM. 2022. Decoupling between soil moisture and biomass drives seasonal variations in live fuel moisture across co-occurring plant functional types. *Fire Ecology* 18: 14.

Cannon AJ. 2018. Multivariate quantile mapping bias correction: an N-dimensional probability density function transform for climate model simulations of multiple variables. *Climate Dynamics* 50: 31–49.

Cardoso AA, Batz TA, McAdam SAM. 2020. Xylem embolism resistance determines leaf mortality during drought in *Persea americana*. *Plant Physiology* 182: 547–554.

Chakroun H, Mouillot F, Hamdi A. 2015. Regional equivalent water thickness modeling from remote sensing across a tree cover/LAI gradient in Mediterranean forests of northern Tunisia. *Remote Sensing* 7: 1937–1961.

Chuvieco E, González I, Verdú F, Aguado I, Yebra M. 2009. Prediction of fire occurrence from live fuel moisture content measurements in a Mediterranean ecosystem. *International Journal of Wildland Fire* 18: 430–441.

Cochard H. 2021. A new mechanism for tree mortality due to drought and heatwaves. *Peer Community Journal* 1: e37.

Cochard H, Pimont F, Ruffault J, Martin-StPaul N. 2021. SurEau: a mechanistic model of plant water relations under extreme drought. *Annals of Forest Science* 78: 55.

Couvreur V, Ledder G, Manzoni S, Way DA, Muller EB, Russo SE. 2018. Water transport through tall trees: a vertically explicit, analytical model of xylem hydraulic conductance in stems. *Plant, Cell & Environment* 41: 1821–1839.

Cruiziat P, Cochard H, Améglio T. 2002. Hydraulic architecture of trees: main concepts and results. *Annals of Forest Science* 59: 723–752.

Dai A. 2013. Increasing drought under global warming in observations and models. *Nature Climate Change* 3: 52–58.

De Cáceres M, Mencuccini M, Martin-StPaul N, Limousin JM, Coll L, Poyatos R, Cabon A, Granda V, Forner A, Valladares F *et al.* 2021. Unravelling the effect of species mixing on water use and drought stress in Mediterranean forests: a modelling approach. *Agricultural and Forest Meteorology* 296: 108233.

De Kauwe MG, Medlyn BE, Ukkola AM, Mu M, Sabot MEB, Pitman AJ, Meir P, Cernusak LA, Rifai SW, Choat B *et al.* 2020. Identifying areas at risk of drought-induced tree mortality across South-Eastern Australia. *Global Change Biology* 26: 5716–5733.

Dennison PE, Moritz MA. 2009. Critical live fuel moisture in chaparral ecosystems: a threshold for fire activity and its relationship to antecedent precipitation. *International Journal of Wildland Fire* 18: 1021–1027.

Duane A, Castellnou M, Brotons L. 2021. Towards a comprehensive look at global drivers of novel extreme wildfire events. *Climatic Change* 165: 43.

Ellis TM, Bowman DMJS, Jain P, Flannigan MD, Williamson GJ. 2022. Global increase in wildfire risk due to climate-driven declines in fuel moisture. *Global Change Biology* 28: 1544–1559.

Fan L, Wigneron J-P, Xiao Q, Al-Yaari A, Wen J, Martin-StPaul N, Dupuy J, Pimont F, Al Bitar A, Fernandez-Moran R *et al.* 2018. Evaluation of microwave remote sensing for monitoring live fuel moisture content in the Mediterranean region. *Remote Sensing of Environment* 205: 210–223.

Gabriel E, Delgado-Dávila R, De Cáceres M, Casals P, Tudela A, Castro X. 2021. Live fuel moisture content time series in Catalonia since 1998. *Annals of Forest Science* 78: 44.

Garnier E, Shipley B, Roumet C, Laurent G. 2001. A standardized protocol for the determination of specific leaf area and leaf dry matter content. *Functional Ecology* 15: 688–695.

Gavinet J, Ourcival JM, Limousin JM. 2019. Rainfall exclusion and thinning can alter the relationships between forest functioning and drought. *New Phytologist* 223: 1267–1279.

van Genuchten MT. 1980. A closed-form equation for predicting the hydraulic conductivity of unsaturated soils. *Soil Science Society of America Journal* 44: 892–898.

Grossiord C, Buckley TN, Cernusak LA, Novick KA, Poulter B, Siegwolf RTW, Sperry JS, McDowell NG. 2020. Plant responses to rising vapor pressure deficit. *New Phytologist* 226: 1550–1566.

Guillemot J, Martin-StPaul NK, Bulascoschi L, Poorter L, Morin X, Pinho BX, le Maire G, PRL B, Oliveira RS, Bongers F *et al.* 2022. Small and slow is safe: on the drought tolerance of tropical tree species. *Global Change Biology* 28: 2622–2638.

Hammond WM, Williams AP, Abatzoglou JT, Adams HD, Klein T, López R, Sáenz-Romero C, Hartmann H, Breshears DD, Allen CD. 2022. Global field observations of tree die-off reveal hotter-drought fingerprint for Earth's forests. *Nature Communications* 13: 1761.

Hammond WM, Yu K, Wilson LA, Will RE, Anderegg WRL, Adams HD. 2019. Dead or dying? Quantifying the point of no return from hydraulic failure in drought-induced tree mortality. *New Phytologist* 223: 1834–1843.

Hölttä T, Cochard H, Nikinmaa E, Mencuccini M. 2009. Capacitive effect of cavitation in xylem conduits: results from a dynamic model. *Plant, Cell & Environment* 32: 10–21.

Jackson RB, Canadell J, Ehleringer JR, Mooney HA, Sala OE, Schulze ED. 1996. A global analysis of root distributions for terrestrial biomes. *Oecologia* 108: 389–411.

Jarvis PG. 1976. The interpretation of the variations in leaf water potential and stomatal conductance found in canopies in the field. *Philosophical Transactions of the Royal Society of London. Series B: Biological Sciences* 273: 593–610.

Jolly M, Hintz J, Linn RL, Kropp RC, Conrad ET, Parsons RA, Winterkamp J. 2016. Seasonal variations in red pine (*Pinus resinosa*) and jack pine (*Pinus banksiana*) foliar physio-chemistry and their potential influence on stand-scale wildland fire behavior. *Forest Ecology and Management* 373: 167–178.

Jolly WM, Hadlow AM, Huguet K. 2014. De-coupling seasonal changes in water content and dry matter to predict live conifer foliar moisture content. *International Journal of Wildland Fire* 23: 480–489.

Jolly WM, Johnson DM. 2018. Pyro-ecophysiology: shifting the paradigm of live wildland fuel research. *Fire* 1: 8.

Jones MW, Abatzoglou JT, Veraverbeke S, Andela N, Lasslop G, Forkel M, Smith AJP, Burton C, Betts RA, van der Werf GR *et al.* 2022. Global and regional trends and drivers of fire under climate change. *Reviews of Geophysics* 60: e2020RG000726.

Karavani A, Boer MM, Baudena M, Colinas C, Díaz-Sierra R, Pemán J, de Luis M, Enríquez-de-Salamanca Á, Resco de Dios V. 2018. Fire-induced deforestation in drought-prone Mediterranean forests: drivers and unknowns from leaves to communities. *Ecological Monographs* 88: 141–169.

Kennedy D, Swenson S, Oleson KW, Lawrence DM, Fisher R, Lola da Costa AC, Gentine P. 2019. Implementing plant hydraulics in the community land model, v.5. *Journal of Advances in Modeling Earth Systems* 11: 485–513.

Klein T, Torres-Ruiz JM, Albers JJ. 2022. Conifer desiccation in the 2021 NW heatwave confirms the role of hydraulic damage. *Tree Physiology* 42: 722–726.

Kotlarski S, Keuler K, Christensen OB, Colette A, Déqué M, Gobiet A, Goergen K, Jacob D, Lüthi D, Van Meijgaard E *et al.* 2014. Regional climate modeling on European scales: a joint standard evaluation of the EURO-CORDEX RCM ensemble. *Geoscientific Model Development* 7: 1297–1333.

Lamarque LJ, Corso D, Torres-Ruiz JM, Badel E, Brodribb TJ, Burlett R, Charrier G, Choat B, Cochard H, Gambetta GA *et al.* 2018. An inconvenient truth about xylem resistance to embolism in the model species for refilling *Laurus nobilis* L. *Annals of Forest Science* 75: 88.

Li L, Yang Z, Matheny AM, Zheng H, Swenson SC, Lawrence DM, Barlage M, Yan B, McDowell NG, Leung LR. 2021. Representation of plant hydraulics in the Noah-MP land surface model: model development and multi-scale evaluation. *Journal of Advances in Modeling Earth Systems* 13: e2020MS002214.

Limousin J-M, Misson L, Lavoir A-V, Martin NK, Rambal S. 2010. Do photosynthetic limitations of evergreen *Quercus ilex* leaves change with long-term increased drought severity? *Plant, Cell & Environment* 33: 863–875.

Limousin JM, Rambal S, Ourcival JM, Rocheteau A, Joffre R, Cortina RR. 2009. Long term transpiration change with rainfall decline in a Mediterranean *Quercus ilex* forest. *Global Change Biology* 15: 2163–2175.

Limousin J-M, Rambal S, Ourcival J-M, Rodríguez-Calcerrada J, Pérez-Ramos IM, Rodríguez-Cortina R, Misson L, Joffre R. 2012. Morphological and phenological shoot plasticity in a Mediterranean evergreen oak facing long-term increased drought. *Oecologia* 169: 565–577.

Limousin J-M, Roussel A, Rodríguez-Calcerrada J, Torres-Ruiz JM, Moreno M, de Jalon LG, Ourcival J-M, Simioni G, Cochard H, Martin-StPaul N. 2022. Drought acclimation of *Quercus ilex* leaves improves tolerance to moderate drought but not resistance to severe water stress. *Plant, Cell & Environment* 45: 1967–1984.

Linn R, Reisner J, Colman JJ, Winterkamp J. 2002. Studying wildfire behavior using FIRETEC. *International Journal of Wildland Fire* 11: 233.

Ma W, Zhai L, Pivovaroff A, Shuman J, Buotte P, Ding J, Christoffersen B, Knox R, Moritz M, Fisher RA *et al.* 2021. Assessing climate change impacts on live fuel moisture and wildfire risk using a hydrodynamic vegetation model. *Biogeosciences* 18: 4005–4020.

Marino E, Yebra M, Guill M, Algeet N, Tom L, Madrigal J, Guijarro M, Hernando C. 2020. Fire-prone shrubland from remote sensing using empirical modelling and RTM simulations. *Remote Sensing* 12: 2251.

Martin-StPaul N, Delzon S, Cochard H. 2017. Plant resistance to drought depends on timely stomatal closure. *Ecology Letters* 20: 1437–1447.

Martin-StPaul N, Pimont F, Dupuy JL, Rigolot E, Ruffault J, Fargeon H, Cabane E, Duché Y, Savazzi R, Toutchkov M. 2018. Live fuel moisture content (LFMC) time series for multiple sites and species in the French Mediterranean area since 1996. *Annals of Forest Science* 75: 1–8.

Martin-Stpaul NK, Limousin JM, Vogt-Schilb H, Rodríguez-Calcerrada J, Rambal S, Longepierre D, Misson L. 2013. The temporal response to drought in a Mediterranean evergreen tree: comparing a regional precipitation gradient and a throughfall exclusion experiment. *Global Change Biology* 19: 2413–2426.

Morin X, Bugmann H, de Coligny F, Martin-StPaul N, Cailleret M, Limousin J-M, Ourcival J-M, Prevosto B, Simioni G, Toigo M *et al.* 2021. Beyond forest succession: a gap model to study ecosystem functioning and tree community composition under climate change. *Functional Ecology* 35: 955–975.

Mouillot F, Rambal S, Lavorel S. 2001. A generic process-based simulator for meditERRanean landscApes (SIERRA): design and validation exercises. *Forest Ecology and Management* 147: 75–97.

Nolan RH, Blackman CJ, de Dios VR, Choat B, Medlyn BE, Li X, Bradstock RA, Boer MM. 2020a. Linking forest flammability and plant vulnerability to drought. *Forests* 11: 779.

Nolan RH, Boer MM, Collins L, Resco de Dios V, Clarke H, Jenkins M, Kenny B, Bradstock RA. 2020b. Causes and consequences of eastern Australia's 2019–2020 season of mega-fires. *Global Change Biology* 26: 1039–1041.

Nolan RH, Boer MM, Resco De Dios V, Caccamo G, Bradstock RA. 2016. Large-scale, dynamic transformations in fuel moisture drive wildfire activity across southeastern Australia. *Geophysical Research Letters* 43: 4229–4238.

Nolan RH, Foster B, Griebel A, Choat B, Medlyn BE, Yebra M, Younes N, Boer MM. 2022. Drought-related leaf functional traits control spatial and temporal dynamics of live fuel moisture content. *Agricultural and Forest Meteorology* 319: 108941.

Nolan RH, Hedo J, Arteaga C, Sugai T, Resco de Dios V. 2018. Physiological drought responses improve predictions of live fuel moisture dynamics in a Mediterranean forest. *Agricultural and Forest Meteorology* 263: 417–427.

Pimont F, Ruffault J, Martin-StPaul NK, Dupuy J-L. 2019a. A cautionary note regarding the use of cumulative burnt areas for the determination of fire danger index breakpoints. *International Journal of Wildland Fire* 28: 254–258.

Pimont F, Ruffault J, Martin-StPaul NK, Dupuy J-L, Pimont F, Ruffault J, Martin-StPaul NK, Dupuy J-L. 2019b. Why is the effect of live fuel moisture content on fire rate of spread underestimated in field experiments in shrublands? *International Journal of Wildland Fire* 28: 127–137.

Pivovaroff AL, Emery N, Rasoul Sharifi M, Witter M, Keeley JE, Rundel PW. 2019. The effect of ecophysiological traits on live fuel moisture content. *Fire* 2: 28.

Rambal S, Ourcival JMJM, Joffre R, Mouillot F, Nouvellon Y, Reichstein M, Rocheteau A, Biology GC, Cedex M, Biology P *et al.* 2003. Drought controls over conductance and assimilation of a Mediterranean evergreen ecosystem: scaling from leaf to canopy. *Global Change Biology* 9: 1813–1824.

Rao K, Williams AP, Diffenbaugh NS, Yebra M, Konings AG. 2022. Plant-water sensitivity regulates wildfire vulnerability. *Nature Ecology & Evolution* 6: 332–339.

Rao K, Williams AP, Flefil JF, Konings AG. 2020. SAR-enhanced mapping of live fuel moisture content. *Remote Sensing of Environment* 245: 111797.

Resco de Dios V, Cunill Camprubí À, Pérez-Zanón N, Peña JC, Martínez del Castillo E, Rodrigues M, Yao Y, Yebra M, Vega-García C, Boer MM. 2022. Convergence in critical fuel moisture and fire weather thresholds associated with fire activity in the pyroregions of Mediterranean Europe. *Science of the Total Environment* 806: 151462.

Resco de Dios VV, Fellows AW, Nolan RH, Boer MM, Bradstock RA, Domingo F, Goulden ML. 2015. A semi-mechanistic model for predicting the moisture content of fine litter. *Agricultural and Forest Meteorology* 203: 64–73.

Rieger M. 1995. Offsetting effects of reduced root hydraulic conductivity and osmotic adjustment following drought. *Tree Physiology* 15: 379–385.

Rodriguez-Dominguez CM, Forner A, Martorell S, Choat B, Lopez R, Peters JMR, Pfautsch S, Mayr S, Carins-Murphy MR, McAdam SAM *et al.* 2022. Leaf water potential measurements using the pressure chamber: synthetic testing of assumptions towards best practices for precision and accuracy. *Plant, Cell & Environment* 45: 2037–2061.

Rossa CG, Veloso R, Fernandes PM. 2016. A laboratory-based quantification of the effect of live fuel moisture content on fire spread rate. *International Journal of Wildland Fire* 25: 569–573.

Ruffault J, Curt T, Martin-StPaul NK, Moron V, Trigo RM. 2018a. Extreme wildfire events are linked to global-change-type droughts in the northern Mediterranean. *Natural Hazards and Earth System Sciences* 18: 847–856.

Ruffault J, Curt T, Moron V, Trigo RM, Mouillot F, Koutsias N, Pimont F, Martin-StPaul NK, Barbero R, Dupuy JL *et al.* 2020. Increased likelihood of heat-induced large wildfires in the Mediterranean Basin. *Scientific Reports* 10: 13790.

Ruffault J, Martin-StPaul N, Pimont F, Dupuy J-LL. 2018b. How well do meteorological drought indices predict live fuel moisture content (LFMC)? An assessment for wildfire research and operations in Mediterranean ecosystems. *Agricultural and Forest Meteorology* 262: 391–401.

Ruffault J, Martin-StPaul NKN, Rambal S, Mouillot F. 2013. Differential regional responses in drought length, intensity and timing to recent climate changes in a Mediterranean forested ecosystem. *Climatic Change* 117: 103–117.

Ruffault J, Pimont F, Cochard H, Dupuy J-L, Martin-StPaul N. 2022. SurEau-Ecos v.2.0: a trait-based plant hydraulics model for simulations of plant water status and drought-induced mortality at the ecosystem level. *Geoscientific Model Development* 15: 5593–5626.

Ruthrof KX, Fontaine JB, Matusick G, Breshears DD, Law DJ, Powell S, Hardy G. 2016. How drought-induced forest die-off alters microclimate and increases fuel loadings and fire potentials. *International Journal of Wildland Fire* 25: 819–830.

Scarff FR, Lenz T, Richards AE, Zanne AE, Wright IJ, Westoby M. 2021. Effects of plant hydraulic traits on the flammability of live fine canopy fuels. *Functional Ecology* 35: 835–846.

Sergent AS, Varela SA, Barigah TS, Badel E, Cochard H, Dalla-Salda G, Delzon S, Fernández ME, Guillemot J, Gyenge J *et al.* 2020. A comparison of five methods to assess embolism resistance in trees. *Forest Ecology and Management* 468: 118175.

Sobol IM. 2001. Global sensitivity indices for nonlinear mathematical models and their Monte Carlo estimates. *Mathematics and Computers in Simulation* 55: 271–280.

Turco M, von Hardenberg J, AghaKouchak A, Llasat MC, Provenzale A, Trigo RM. 2017. On the key role of droughts in the dynamics of summer fires in Mediterranean Europe. *Scientific Reports* 7: 81.

Tuzet A, Granier A, Betsch P, Peiffer M, Perrier A. 2017. Modelling hydraulic functioning of an adult beech stand under non-limiting soil water and severe drought condition. *Ecological Modelling* 348: 56–77.

Tyree MT, Hammel HT. 1972. The measurement of the turgor pressure and the water relations of plants by the pressure-bomb technique. *Journal of Experimental Botany* 23: 267–282.

Tyree MT, Yang S. 1990. Water-storage capacity of Thuja, Tsuga and Acer stems measured by dehydration isotherms. *Planta* 182: 420–426.

Vidal JP, Martin E, Franchistéguy L, Baillon M, Soubeyroux JM. 2010. A 50-year high-resolution atmospheric reanalysis over France with the Safran system. *International Journal of Climatology* 30: 1627–1644.

Yebra M, Dennison PE, Chuvieco E, Riaño D, Zylstra P, Hunt ER, Danson FM, Qi Y, Jurdao S. 2013. Remote sensing of environment a global review of remote sensing of live fuel moisture content for fire danger assessment: moving towards operational products. *Remote Sensing of Environment* 136: 455–468.

Yebra M, Quan X, Riaño D, Rozas Larraondo P, van Dijk AIJM, Cary GJ. 2018. A fuel moisture content and flammability monitoring methodology for continental Australia based on optical remote sensing. *Remote Sensing of Environment* 212: 260–272.

Yebra M, Scortechini G, Badi A, Beget ME, Boer MM, Bradstock R, Chuvieco E, Danson FM, Dennison P, Resco de Dios V *et al.* 2019. Globe-LFMC, a global plant water status database for vegetation ecophysiology and wildfire applications. *Scientific Data* 6: 155.

Supporting Information

Additional Supporting Information may be found online in the Supporting Information section at the end of the article.

Table S1 List of model parameters and values used in *SurEau-Ecos-FMC* to simulate the dynamics of fuel moisture content in a *Quercus ilex* forest stand.

Please note: Wiley is not responsible for the content or functionality of any Supporting Information supplied by the authors. Any queries (other than missing material) should be directed to the *New Phytologist* Central Office.